Efficient, high-power, ytterbium-fiber-laser-pumped picosecond optical parametric oscillator

O. Kokabee,[1,*] A. Esteban-Martin,[1] and M. Ebrahim-Zadeh[1,2]

[1]*ICFO–Institut de Ciencies Fotoniques, Mediterranean Technology Park, 08860 Castelldefels, Barcelona, Spain*

[2]*Institucio Catalana de Recerca i Estudis Avancats (ICREA), Passeig Lluis Companys 23, Barcelona 08010, Spain*

**Corresponding author: omid.kokabee@icfo.es*

Received June 30, 2010; revised August 6, 2010; accepted August 20, 2010;
posted September 7, 2010 (Doc. ID 130670); published September 21, 2010

We report a high-power picosecond optical parametric oscillator (OPO) synchronously pumped by a Yb fiber laser at 1.064 μm, providing 11.7 W of total average power in the near to mid-IR at 73% extraction efficiency. The OPO, based on a 50 mm MgO:PPLN crystal, is pumped by 20.8 ps pulses at 81.1 MHz and can simultaneously deliver 7.1 W of signal at 1.56 μm and 4.6 W of idler at 3.33 μm for 16 W of pump power. The oscillator has a threshold of 740 mW, with maximum signal power of 7.4 W at 1.47 μm and idler power of 4.9 W at 3.08 μm at slope efficiencies of 51% and 31%, respectively. Wavelength coverage across 1.43–1.63 μm (signal) and 4.16–3.06 μm (idler) is obtained, with a total power of ~11 W and an extraction efficiency of ~68%, with pump depletion of ~78% maintained over most of the tuning range. The signal and idler output have a single-mode spatial profile and a peak-to-peak power stability of ±1.8% and ±2.9% over 1 h at the highest power, respectively. A signal pulse duration of 17.3 ps with a clean single-peak spectrum results in a time-bandwidth product of ~1.72, more than four times below the input pump pulses.

OCIS codes: 190.7110, 190.4970, 160.3730, 320.5390.

Synchronously pumped optical parametric oscillators (OPOs) are versatile sources of tunable high-repetition-rate ultrashort pulses in spectral regions inaccessible to mode-locked lasers. In picosecond (ps) operation, such OPOs are of particular interest for applications where high average powers and a compromise between short pulse durations and narrow spectral bandwidths are required [1,2]. An important factor in the development of ps OPOs is the exploitation of practical high-power ps laser pump sources. Mode-locked Nd:YAG lasers near 1.06 μm have, in the past, provided viable pumping platforms for ps OPOs [3–6] but suffer from large size, bulkiness, and lack of simplicity, even in diode-pumped configurations. For further progress in ps OPOs, it is desirable to minimize system size, complexity, and cost while maintaining or enhancing overall device performance with regard to all-important operating parameters. One strategy to achieve this goal is the exploitation of mode-locked fiber lasers, providing unprecedented optical powers and high temporal, spectral, and spatial beam quality with highly competitive performance capabilities but in far more simplified, robust, compact, portable, and cost-effective architectures. Fiber lasers also offer increased immunity from environmentally induced thermal effects over bulk solid-state lasers, resulting in overall improvement in OPO output stability.

Another pivotal factor in the realization of practical ps OPOs is the exploitation of suitable nonlinear materials capable of withstanding the large average powers while providing long interaction lengths under noncritical interaction for maximum nonlinear gain, and extended phase matching over wavelength regions of interest. Such simultaneous requirements are met uniquely by quasi-phase-matched (QPM) nonlinear crystals. Among them, periodically poled $LiNbO_3$ (PPLN) with high nonlinearity ($d_{\mathrm{eff}} \sim 17$ pm/V), long interaction lengths (up to 80 mm), and transparency up to ~5 μm has been established as the most effective material at high average powers in the IR [6]. PPLN is susceptible to photorefractive damage when exposed to high levels of near-IR light, resulting in the generation of significant non-phase-matched visible radiation, which can lead to output power degradation and instability. However, heating the crystal to above 150 °C or doping with MgO [7,8] can effectively overcome this problem.

In earlier work, a PPLN-based OPO driven by 270 fs pulses at 54 MHz from a femtosecond Yb fiber laser was reported with a maximum average signal power of 90 mW in 330 fs pulses over the 1.55–1.95 μm range for 410 mW of pump power [9]. Later, a ps OPO based on MgO:PPLN pumped by 437 fs pulses from an Yb fiber laser at 15.3 MHz was demonstrated [10], providing 1.5 ps signal pulses over the 1.42–1.56 μm range with a maximum average power of 1.09 W at 17% extraction efficiency for 6.4 W of pump power. More recently, an MgO:PPLN ps OPO pumped by a fiber-amplified gain-switched laser diode at 114.8 MHz was reported [11], providing 17 ps signal pulses over the 1.4–1.7 μm range with a maximum average power of 7.3 W at 1.54 μm and 3.1 W at 3.4 μm at 43.3% total extraction efficiency for 24 W of pump power. Here, we report efficient and stable operation of a Yb-fiber-laser-pumped ps OPO based on MgO:PPLN at multiwatt signal and idler power levels with much improved extraction efficiency. We extract a total average power of up to 11.7 W (7.1 W of signal at 1.56 μm and 4.6 W of idler at 3.33 μm) at 73% extraction efficiency in high spectral and spatial beam quality with excellent output power stability.

A schematic of the experimental setup is shown in Fig. 1. The pump source was a passively mode-locked ps Yb fiber laser (Fianium, FemtoPower FP1060-20), delivering up to 20 W of average power at 81.1 MHz at 1.064 μm. The pump pulses had a duration of 20.8 ps (FWHM) and a double-peak spectrum with a bandwidth of 1.38 nm (FWHM), resulting in a time-bandwidth product of $\Delta\tau\Delta\nu \sim 7.6$, many times the transform limit. The 5 mol.% MgO:PPLN crystal (HC Photonics, Taiwan)

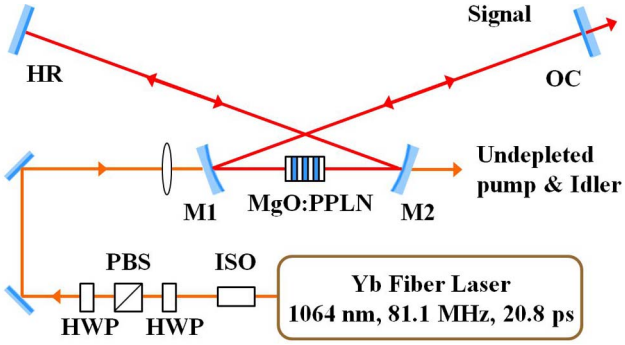

Fig. 1. (Color online) Configuration of the ps OPO synchronously pumped by a mode-locked Yb fiber laser: ISO, optical isolator; HWP, half-wave plate; PBS, polarizing beam splitter. First HWP and PBS are used for power attenuation, while the second HWP is used to rotate the pump beam polarization.

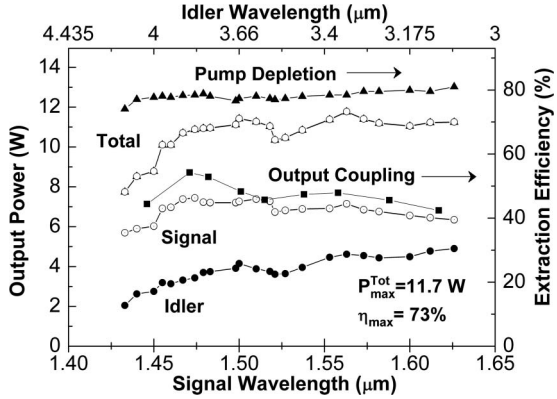

Fig. 3. OPO power performance, pump depletion, and output coupling values in the OPO tuning range from 1.43 to 1.63 μm for the signal and from 3.06 to 4.16 μm for the idler.

was 50 mm long and 1 mm thick, with five gratings, ranging in period from 28.5 to 30.5 μm. The crystal faces were antireflection coated for signal ($R < 1\%$ over the range of 1.45–1.75 μm), with high transmission for pump ($T > 97\%$) and idler ($T > 95.5\%$ over 3–4.2 μm). The crystal was housed in an oven with a stability of ± 0.1 °C, and its temperature could be adjusted from room temperature to 200 °C. The pump was focused to a beam waist radius of ~45 μm at the center of the crystal, resulting in a focusing parameter of $\xi \sim 1.94$. The OPO cavity was a four-mirror standing wave, comprising two concave mirrors with CaF_2 substrates (M1 and M2, $r = 20$ cm) and a plane mirror (HR), all highly reflecting for signal ($R > 99.9\%$ over 1.4–1.7 μm) and highly transmitting for pump ($T \sim 92\%$) and idler ($T > 80\%$ over 3–4.2 μm). The signal output was extracted through a plane output coupler (OC), while the idler and undepleted pump were measured after M2. The cavity configuration resulted in a signal beam waist radius of ~54 μm inside the crystal, providing optimum overlap with the pump (b_p–b_s).

We investigated power scaling of the OPO by deploying a wide range of output couplers for the signal from ~3% to ~55%. Figure 2 shows the average signal and idler output powers extracted from the OPO versus the pump power at the input to the crystal. The data were obtained at a 1.47 μm (signal) and 3.08 μm (idler), corresponding to the output coupling of ~55% and ~42%,

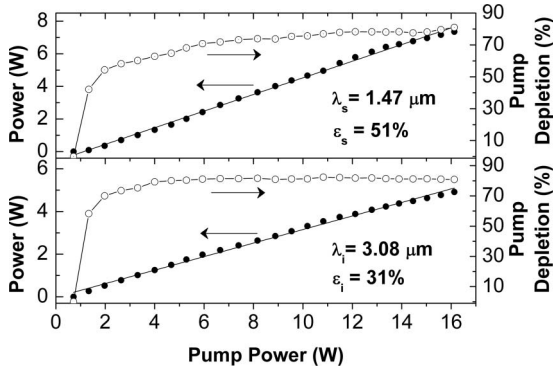

Fig. 2. Extracted signal and idler average power and corresponding pump depletion as a function of input pump power at 1.47 and 3.08 μm, respectively. ε_s and ε_i are external slope efficiencies.

respectively, for which maximum power was obtained in each case for the highest input power. Because of ~20% overall loss through the optical isolator and transmission optics, the maximum pump power at the input to the crystal was 16 W. The signal and idler output power increase linearly with pump power with external slope efficiencies of 51% and 31%, respectively, reaching 7.4 and 4.9 W at 16 W of pump. Also shown in Fig. 2 is the pump depletion, which in both cases increases rapidly at lower powers, before reaching ~82% and remaining almost constant up to the maximum input pump power. The average pump power threshold for the OPO is 740 mW.

Wavelength tuning was achieved by varying the crystal temperature for different grating periods, resulting in signal coverage over 1.43–1.63 μm and corresponding idler range over 4.16–3.06 μm. Figure 3 shows the average signal, idler, and total power, and the corresponding extraction efficiency, pump depletion, and output coupling across the tuning range at 16 W of pump power. Because of wavelength dependence, the output coupler transmission varies from ~44% at the shortest signal wavelength of 1.43 μm to ~55% at 1.47 μm and then decreases to ~42% at 1.63 μm. The signal output power and efficiency closely follow the output coupling with a maximum power of 7.4 W at 1.47 μm for the highest output coupling of 55%. The signal output power and extraction efficiency still remain at ~7 W and ~43% over almost the entire tuning range, except below 1.45 μm due to the rise in the reflection losses of crystal coatings (from 0.5% to 1%). Similarly, with the increased crystal coating losses at longer idler wavelengths (from 2.6% at 3.1 μm to 4.5% at 4.2 μm), idler power also experiences a drop, with the highest output power of 4.9 W at 3.08 μm, and more than 2 W available at 4.16 μm. The combined signal and idler power remains at ~11 W across most of the tuning range at ~68% extraction efficiency, except below 1.45 μm, with a nearly constant pump depletion of ~78%. The extraction efficiency of ~68% is very close to the pump depletion of ~78%, implying that the total obtained power is already very close to the maximum attainable output from the device. The highest total average power is 11.7 W, obtained at 1.56 μm, with a corresponding extraction efficiency of 73%.

Temporal measurements of signal pulses were performed using two-photon intensity autocorrelation.

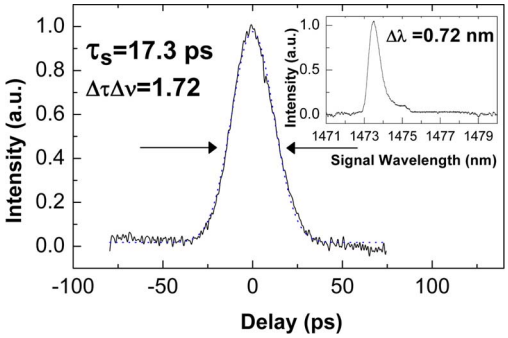

Fig. 4. (Color online) Typical intensity autocorrelation with the sech^2 fit (dotted line) and corresponding optical spectrum of OPO signal pulses at 1.47 μm at 7.4 W average output power.

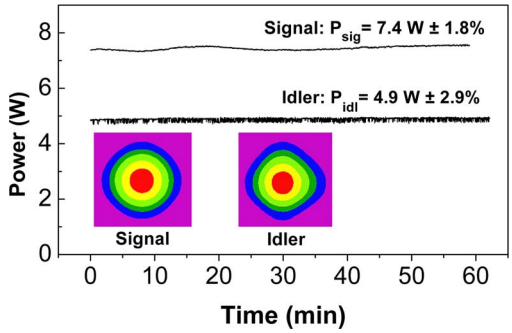

Fig. 5. (Color online) Signal and idler power stability over time and corresponding spatial beam profiles at 1.47 and 3.08 μm, respectively, and at maximum output power.

Figure 4 shows a typical intensity autocorrelation and spectrum at 1.47 μm, where the OPO delivered the highest signal power. The deconvolved FWHM pulse duration is 17.3 ps (assuming a sech^2 pulse shape). The spectrum is a clean single peak with an FWHM bandwidth of 0.72 nm, resulting in a time-bandwidth product of 1.72. This is nearly 4.5 times lower than the value of 7.6 for the pump pulses. The substantial reduction in signal bandwidth is due to the narrow spectral acceptance of the long crystal used in our experiment. The spectral acceptance bandwidth of MgO:PPLN varies from ~1.8 nm.cm at 1.43 μm to ~1.5 nm.cm at 1.63 μm, resulting in 0.3–0.36 nm for the 50 mm crystal, thus leading to the bandwidth reduction and spectral cleaning from the double-peak pump to a smooth single-peak signal. Further reductions in signal bandwidth can also be obtained by using frequency selection elements, such as intracavity etalons [6], which will result in time-bandwidth products closer to the transform limit.

The power stability of the signal at 1.47 μm and idler at 3.08 μm at the highest input pump power are shown in Fig. 5. The MgO:PPLN crystal and the concave mirrors (M1 and M2) were isolated from laboratory air by an enclosure in a Perspex box with four openings to allow entrance of the input pump beam and extraction of signal, idler, and the undepleted pump. The signal and idler exhibited excellent passive peak-to-peak power stability of $\pm 1.8\%$ at 7.4 W and $\pm 2.9\%$ at 4.9 W over 1 h, respectively. The stability could be further enhanced by more stringent mechanical and thermal isolation of the system using better mirror mounts and improved oven design to minimize the air flow over the crystal. The measured spatial profile of the signal and idler beams at 1.47 and 3.08 μm, respectively, is shown in the inset of Fig. 5. Both are characterized by single-mode profile at their highest output power.

This research was supported by the European Union (EU) 7th Framework Program through project MIRSURG (224042) and by the European Office of Aerospace Research and Development (EOARD) through grant FA8655-09-1-3017. We also acknowledge support by the Ministry Science and Innovation (Spain) through the Consolider project SAUUL (CSD2007-00013).

References

1. W. Patterson, S. Bigotta, M. Sheik-Bahae, D. Parisi, M. Tonelli, and R. Epstein, Opt. Express **16**, 1704 (2008).
2. A. Baron, A. Ryasnyanskiy, N. Dubreuil, Ph. Delaye, Q. Vy Tran, S. Combrié, A. de Rossi, R. Frey, and G. Roosen, Opt. Express **17**, 552 (2009).
3. J. Chung and A. Siegman, J. Opt. Soc. Am. B **10**, 2201 (1993).
4. B. Ruffing, A. Nebel, and R. Wallenstein, Appl. Phys. B **67**, 537 (1998).
5. K. Finsterbusch, R. Urschel, and H. Zacharias, Appl. Phys. B **70**, 741 (2000).
6. C. W. Hoyt, M. Sheik-Bahae, and M. Ebrahimzadeh, Opt. Lett. **27**, 1543 (2002).
7. D. A. Bryan, R. Gerson, and H. E. Tomaschke, Appl. Phys. Lett. **44**, 847 (1984).
8. Y. Furukawa, K. Kitamura, S. Takekawa, A. Miyamoto, M. Terao, and N. Suda, Appl. Phys. Lett. **77**, 2494 (2000).
9. M. V. O'Connor, M. A. Watson, D. P. Shepherd, D. C. Hanna, J. H. V. Price, A. Malinowski, J. Nilsson, N. G. R. Broderick, D. J. Richardson, and L. Lefort, Opt. Lett. **27**, 1052 (2002).
10. T. P. Lamour, L. Kornaszewski, J. H. Sun, and D. T. Reid, Opt. Express **17**, 14229 (2009).
11. F. Kienle, K. K. Chen, S. Alam, C. B. E. Gawith, J. I. Mackenzie, D. C. Hanna, D. J. Richardson, and D. P. Shepherd, Opt. Express **18**, 7602 (2010).